

THE SCIENTIFIC CASE FOR SPECTROPOLARIMETRY FROM SPACE:
A NOVEL DIAGNOSTIC WINDOW ON COSMIC MAGNETIC FIELDS

J. Trujillo Bueno^{1,2}, E. Landi Degl’Innocenti³, R. Casini⁴ and V. Martínez Pillet¹

¹Instituto de Astrofísica de Canarias, 38205 La Laguna, Tenerife, Spain

²Consejo Superior de Investigaciones Científicas, Spain

³Dipartimento di Astronomia e Scienza dello Spazio, Largo E. Fermi 2, I-50125 Firenze, Italy

⁴High Altitude Observatory, P. O. Box, Boulder CO 80307-3000, USA

ABSTRACT

One of the greatest future challenges in cosmic physics is the empirical investigation of the magnetic field vector in a variety of astrophysical plasmas, including the solar corona. The chances of attaining this goal would be dramatically increased if we could carry out spectropolarimetric observations from space in order to measure the polarization signals that scattering processes induce in permitted UV/EUV spectral lines, such as those of the Lyman series of hydrogen. The physical interpretation of this type of observations would allow us to infer the magnetic field vector via the Hanle effect, which consists in the modification of scattering polarization signals due to the presence of a magnetic field. In particular, the Hanle effect either in forward scattering or at 90° scattering is a unique and powerful tool for the “measurement” of magnetic fields in the solar transition region and corona. Here we highlight the great diagnostic potential of spectropolarimetry and argue that ESA should take advantage of the present European leadership in this field to open this new diagnostic window on the Universe.

Key words: Polarization – Scattering – Sun: magnetic fields – Stars: magnetic fields – Astrophysical Plasmas: magnetic fields

1. INTRODUCTION

In our opinion, the greatest future challenge in space astrophysics is the empirical investigation of the magnetic field in a variety of astrophysical systems, such as the solar corona, circumstellar envelopes, accreting systems, etc. In particular, if we really want to understand how the solar system works, we also need to decipher the 3D magnetic structure of the solar outer atmosphere, from the microscopic to the macroscopic scales. In fact, the magnetic field is the most important physical quantity that practically controls everything interesting happening in the Sun (e.g., the million-degree corona, irradiance variations, explosive events like coronal mass ejections which dramatically influence the heliosphere in which *all* solar-system planets are embedded, etc.).

In order to make progress in our understanding we need to make *new* measurements, especially of those phys-

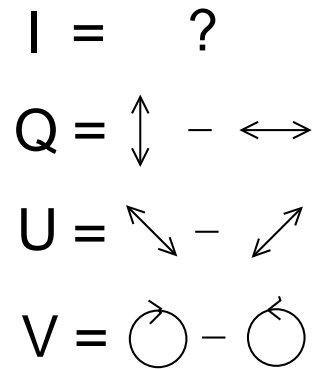


Figure 1. Pictorial definition of the Stokes parameters. The observer is facing the radiation source. The Stokes $Q(\lambda)$ profile is the intensity difference between vertical and horizontal linear polarization, Stokes $U(\lambda)$ the intensity difference between linear polarization at +45° and -45°, while Stokes $V(\lambda)$ the intensity difference between right- and left-handed circular polarization (cf. Born & Wolf 1994; Landi Degl’Innocenti & Landolfi 2004). The panel with the Stokes I parameter shows a question mark in order to point out that Stokes I can be defined in the same way as Stokes Q , U or V , but with a ‘+’ sign instead of a ‘-’ sign.

ical quantities that remain basically unknown, like the magnetic field. To this end we need to carry out spectropolarimetric observations from space, throughout the whole electromagnetic spectrum, but especially in the UV, EUV and X-ray spectral regions. Figure 1 summarizes the definition of the Stokes parameters, which characterize the state of polarization of a quasi-monochromatic beam of electromagnetic radiation.

The polarization signals we are thinking of are mainly those produced by scattering processes in spectral lines. Such linear polarization signals are sensitive to magnetic fields in a parameter domain that goes from field intensities as low as one milligauss to hundreds of gauss (Hanle effect). Observations of these polarization effects provide key information, impossible to obtain via conventional spectroscopy.

For instance, Fig. 2 contrasts the Fraunhofer spectrum (i.e., the visible intensity spectrum of the Sun with its multitude of absorption lines) with the so-called *second solar spectrum* (Stenflo & Keller 1996), which is the linearly polarized spectrum produced by scattering processes

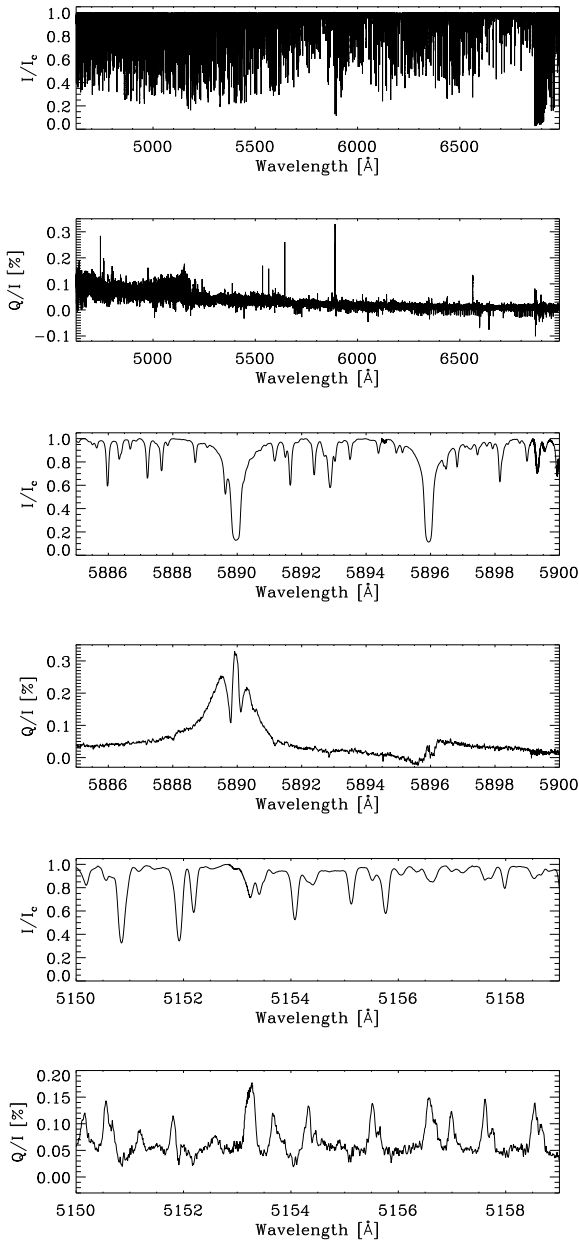


Figure 2. The Fraunhofer spectrum (displayed as normalized intensity of the continuum, I/I_c) versus the “second solar spectrum” (displayed as fractional linear polarization, Q/I). The positive reference direction for the Stokes Q parameter is the parallel to the observed solar limb.

in the solar atmosphere. The observations of Fig. 2 were carried out by Gandorfer (2000) with the Zürich Imaging Polarimeter (ZIMPOL) at the Istituto Ricerche Solari Locarno (Switzerland). The spectrograph’s slit was located parallel to the solar limb and at only 5 arcseconds from it. The first two panels (counting from top to bottom) show the whole visible region of the solar spectrum, while the remaining panels are enlarged portions around selected wavelengths. Thus, the fourth panel shows the complex

Q/I structure across the sodium doublet, while the bottom panel demonstrates that C_2 molecules in the quiet solar photosphere are very active in producing scattering polarization signals. As seen in the figure, the second solar spectrum has a structural richness that often exceeds that of the ordinary intensity spectrum on which most of our astrophysics is based on. It is also of interest to note that the scattering polarization amplitudes tend to increase towards the blue and near-UV regions of the Fraunhofer spectrum. For example, in the spectral region between 3910 Å and 4630 Å (see Gandorfer 2002) we find spectral lines with Q/I signals as large as 3%, such as that of Ca I at 4227 Å. The physical understanding and theoretical modeling of the second solar spectrum has led to new insights on scattering physics and the hidden magnetism of the solar atmosphere (e.g., Trujillo Bueno & Landi Degl’Innocenti 1997; Landi Degl’Innocenti 1998; Manso Sainz & Trujillo Bueno 2003; Trujillo Bueno et al. 2002a,b; 2004).

It would be of great scientific interest to put a high-sensitivity polarimeter in a space telescope in order to simply *discover* how the linearly polarized spectrum of a diverse variety of astrophysical objects looks like. Actually, we should not forget that unpolarized radiation can be expected *only* from a perfectly symmetric object. Therefore, spectropolarimetry and imaging polarimetry may also help us to infer the geometry of the astrophysical object under investigation, even when it is impossible to resolve it spatially.

The primary emission of the 10^6 K solar coronal plasma is in the UV, EUV and soft X-ray regions of the spectrum, which can only be observed from space. This paper emphasizes the diagnostic potential of scattering polarization and the Hanle effect in permitted UV lines for the empirical investigation of the magnetic field vector in the solar outer atmosphere (chromosphere, transition region and corona). As we shall see, this is the most promising tool we have for mapping the strength and orientation of the coronal magnetic field. Obviously, the required observations can be realized only from a UV/EUV spectropolarimeter on board of a space telescope.

The outline of this paper is the following. After pointing out in Section 2 the advantages and disadvantages of the Zeeman effect, we turn our attention to explaining in Section 3 what the Hanle effect is and why it offers a very attractive diagnostic window on astrophysical magnetic fields¹. Our arguments in this respect are made more specific in Section 4, since there we show theoretical model calculations of the Hanle effect in the Lyman α line, both

¹ The reader interested mainly in the basic idea of the diagnostic tool may skip the three subsections on the quantum description of the Hanle effect, which are included only to provide a deeper insight on this fascinating effect which has found so many applications in physics (e.g., Moruzzi & Strumia 1991).

for the 90° and forward scattering cases. Finally, Section 5 summarizes our main conclusions and recommendations.

2. THE ZEEMAN EFFECT

As illustrated in Fig. 3, the Zeeman effect requires the presence of a magnetic field, which causes the atomic and molecular energy levels to split into different magnetic sublevels characterized by their magnetic quantum number M . Each level of total angular momentum J splits into $(2J + 1)$ sublevels, the splitting being proportional to the level's Landé factor, g_J , and to the magnetic field strength. As a result, a spectral line due to a transition between a lower level with (J_l, g_l) and an upper level with (J_u, g_u) is composed of several individual components whose frequencies are given by $\nu_{J_l M_l}^{J_u M_u} = \nu_0 + \nu_L(g_u M_u - g_l M_l)$, where ν_0 is the frequency of the line in the absence of magnetic fields and $\nu_L = 1.3996 \times 10^6 B$ is the Larmor frequency (with B the magnetic field strength expressed in gauss).

The important point to remember is that the polarization signals produced by the Zeeman effect are caused by the *wavelength shifts* between the π ($\Delta M = M_u - M_l = 0$) and $\sigma_{b,r}$ ($\Delta M = \pm 1$) transitions.

The good news about the Zeeman effect is that the mere detection of polarization implies the presence of a magnetic field. The bad news are the following:

- It is of limited practical interest for the determination of magnetic fields in hot coronal plasmas because the Zeeman polarization scales with the ratio between the Zeeman splitting and the Doppler-broadened line width.
- The Zeeman effect is *blind* to magnetic fields that have mixed polarities at sub-resolution scales.

3. THE HANLE EFFECT

Scattering processes in spectral lines produce linear polarization signals, even in the absence of magnetic fields. The amplitude and orientation of the linear polarization of the scattered light are modified in the presence of a magnetic field *inclined* with respect to the symmetry axis of the incident radiation field. This is the so-called Hanle effect (e.g., Trujillo Bueno 2001, for an overview on both the classical and quantum descriptions).

The Hanle effect (Hanle 1924) played a fundamental role in the development of quantum mechanics because it led to the introduction and clarification of the concept of coherent superposition of pure states (Bohr 1924; Heisenberg 1925). This effect is directly related to the generation of coherent superposition of degenerate Zeeman sublevels of an atom or molecule by a light beam. As the Zeeman sublevels are split by the magnetic field, the degeneracy is lifted and the quantum coherences are modified. This gives rise to a characteristic magnetic-field dependence of the

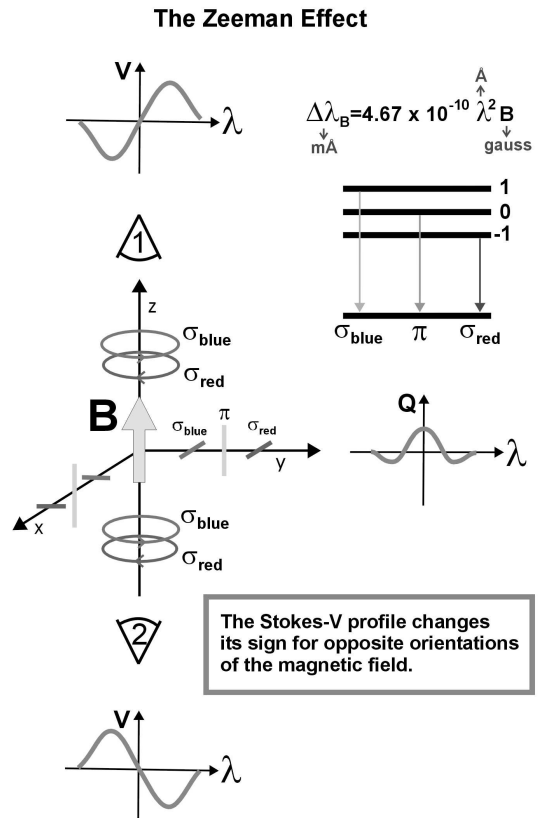


Figure 3. The oscillator model for the Zeeman effect indicating the characteristic shapes of the circular and linear polarization profiles as generated locally via the emission process. It is important to note that the Stokes $V(\lambda)$ profile changes its sign for opposite orientations of the magnetic field vector, while the Stokes $Q(\lambda)$ profile reverses sign when the transverse field component is rotated by $\pm 90^\circ$.

linear polarization of the scattered light that is finding increasing application as a diagnostic tool for magnetic fields in astrophysics (e.g., Asensio Ramos et al. 2005; Casini et al. 2003; Trujillo Bueno et al. 2002a,b; 2004).

In order to highlight the diagnostic potential of the Hanle effect we consider scattering processes in a $J_l = 0 \rightarrow J_u = 1$ line transition for the following two geometries: 90° scattering and forward scattering.

3.1. 90° SCATTERING

Figure 4 illustrates the 90° scattering case, in the absence and in the presence of a magnetic field. For this geometry the largest polarization amplitude occurs for the zero field reference case, with the direction of the linear polarization as indicated in the top panel (i.e, perpendicular to the scattering plane).

The two lower panels illustrate what happens when the scattering processes take place in the presence of a magnetic field pointing (a) towards the observer (left panel)

or (b) away from him/her (right panel). In both situations the polarization amplitude is *reduced* with respect to the previously discussed unmagnetized case. Moreover, the direction of the linear polarization is *rotated* with respect to the zero field case. Typically, this rotation is *counter-clockwise* for case (a), but *clockwise* for case (b)². Therefore, when opposite magnetic polarities coexist within the spatio-temporal resolution element of the observation the direction of the linear polarization is the same as in the top panel of Fig. 4, simply because the rotation effect cancels out. However, the polarization amplitude is indeed reduced with respect to the zero field reference case, which provides an “observable” that can be used for obtaining empirical information on hidden, mixed polarity fields at subresolution scales in the solar atmosphere (Stenflo 1994; Trujillo Bueno et al. 2004).

Other examples of magnetic field diagnostics based on the Hanle effect for the 90° scattering case can be seen in Bommier et al. (1994), Casini et al. (2003), Merenda et al. (2005) and Trujillo Bueno et al. (2002a; 2005).

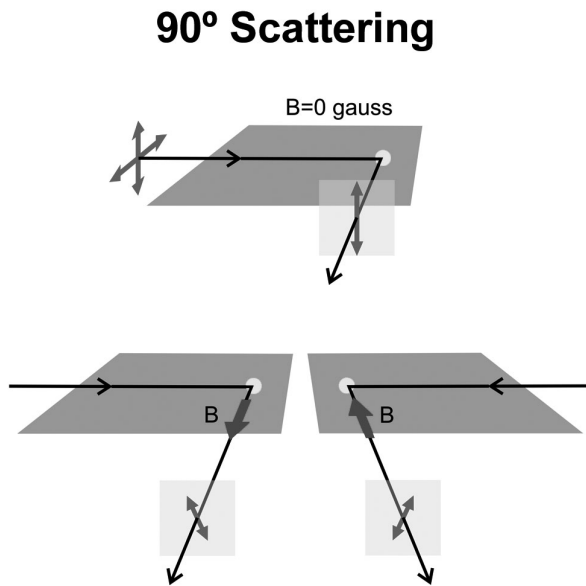


Figure 4. The 90° scattering case in the absence (top panel) and in the presence (bottom panels) of a deterministic magnetic field.

3.2. FORWARD SCATTERING

Figure 5 illustrates the case of forward scattering, in the absence and in the presence of a magnetic field. In this geometry we have *zero* polarization for the unmagnetized reference case, while the largest linear polarization (ori-

² This occurs when the Landé factor, g_L , of the transition’s upper level is positive, while the opposite behavior takes place if $g_L < 0$.

ented along the direction of the external magnetic field) is found for “sufficiently strong” fields (i.e., for a magnetic strength such that the ensuing Zeeman splitting is much larger than the level’s natural width).

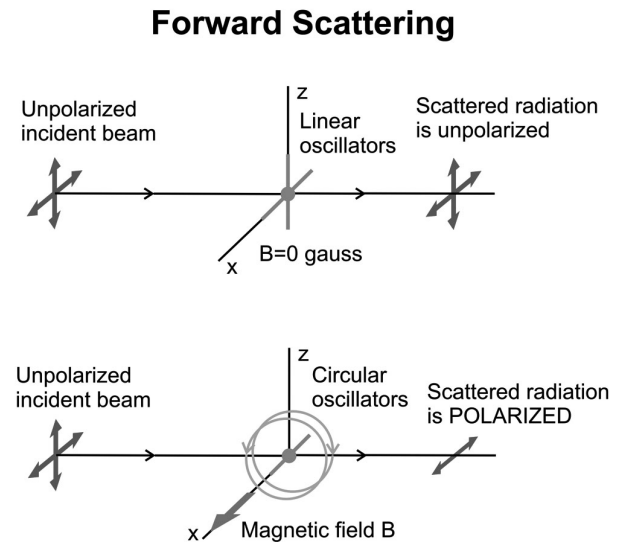


Figure 5. The forward scattering case, in the absence (top panel) and in the presence (bottom panel) of a deterministic magnetic field.

In other words, in the presence of an *inclined* magnetic field that breaks the symmetry of the scattering polarization problem, forward scattering processes can produce linear polarization signals in spectral lines. In this case, the linear polarization is *created* by the Hanle effect, a physical phenomenon that has been clearly demonstrated via spectropolarimetry of solar coronal filaments in the He I 10830 Å multiplet (Trujillo Bueno et al. 2002a). Additional examples of magnetic field diagnostics that make use of forward scattering polarization signals can be seen in Collados et al. (2003), Lagg et al. (2004) and Solanki et al. (2003).

Finally, in Fig. 6 we show that, depending on the scattering geometry, the Hanle effect can either depolarize (case of the solar limb; $\mu = 0.1$) or polarize (case of disk center; $\mu = 1$).

3.3. THE CRITICAL MAGNETIC FIELD

The basic formula of the Hanle effect is the following³:

$$B_H \approx 1.137 \times 10^{-7} / (t_{\text{life}} g_L), \quad (1)$$

where $t_{\text{life}} \approx 1/A_{ul}$ (being A_{ul} the Einstein coefficient for the spontaneous emission process) is the lifetime (in seconds) of the upper level of the spectral line transition under consideration and g_L its Landé factor. This expression

³ This formula results from equating the Zeeman splitting of the atomic or molecular level under consideration (i.e., $2\pi\nu_L g_L$) with the level’s natural width (i.e., $1/t_{\text{life}}$)

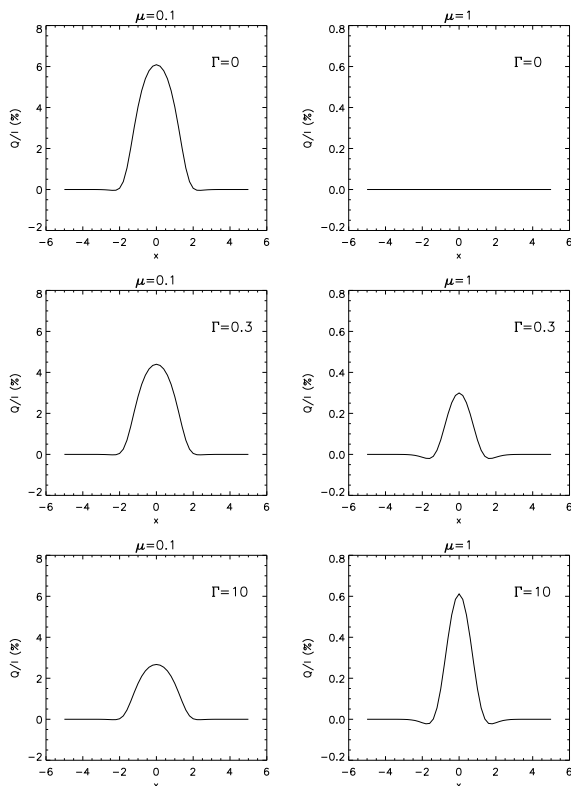


Figure 6. Hanle-effect radiative transfer simulation in a schematic solar model atmosphere, assuming a two-level atomic model with $J_l = 0$ and $J_u = 1$ and neglecting depolarizing collisions. The figure shows the emergent fractional linear polarization versus the line frequency in units of the Doppler width. The magnetic field is parallel to the stellar surface, while the simulated polarimetric observations are for line of sights with $\mu = \cos \theta = 0.1$ (the solar limb case) and $\mu = \cos \theta = 1$ (the disk center case), with θ the heliocentric angle. Both line of sights are perpendicular to the assumed horizontal field, whose intensity is quantified by $\Gamma = 8.79 \times 10^6 B g_J / A_{ul}$, with $g_J = 1$, the magnetic strength B expressed in gauss and the Einstein A_{ul} -coefficient in s^{-1} .

allows us to estimate the critical magnetic field strength B_H (in gauss) for which one may expect a sizable change of the scattering polarization signal with respect to the unmagnetized reference case. This formula provides a reliable estimation *only* when radiative transitions dominate completely the atomic excitation. If elastic and/or inelastic collisions are also efficient, then the critical field increases, since it turns out to be approximately given by (Trujillo Bueno 2003b)

$$B \approx \frac{1 + \delta(1 - \epsilon)}{1 - \epsilon} B_H, \quad (2)$$

where $\delta = D/A_{ul}$ quantifies the rate of elastic (depolarizing) collisions in units of the Einstein A_{ul} -coefficient, and $\epsilon = C_{ul}/(C_{ul} + A_{ul})$ is the probability that a de-excitation event is caused by collisions (with C_{ul} the rate of inelastic

collisional transitions between the upper level “ u ” and the lower level “ l ”).

3.4. THE QUANTUM DESCRIPTION: ATOMIC POLARIZATION

The description of the Hanle effect given in Figs. 4 and 5 is based on the classical oscillator model, which holds for the particular case of a triplet line transition (i.e., with $J_u = 1$, $J_l = 0$ and spin $S = 0$). For treating more complex atomic systems we need to work within the framework of the quantum theory of polarization. In this and the following subsections we are going to introduce only the basic ingredients of the quantum theory of the Hanle effect, hoping that our presentation without equations will motivate the reader to go deeper into the subject (e.g., by reading the book *Polarization in Spectral Lines*, by Landi Degl’Innocenti & Landolfi 2004).

As mentioned in Section 2, if there is no Zeeman splitting there is no wavelength shift between the π and σ transitions. Accordingly, one might think that there is no measurable polarization because the polarizations of such components cancel out. However, it is easy to see that this is only true if the populations of the individual magnetic sublevels pertaining to the lower and/or upper levels of the spectral line under consideration are assumed to be identical. To this end, consider the case of a line transition with $J_l = 0$ and $J_u = 1$ and choose the quantization axis of total angular momentum along the solar radius vector through the observed point. Assume that the population of the upper-level magnetic sublevel with $M_u = 0$ is *smaller* than the populations of the magnetic sublevels with $M_u = \pm 1$. As a result, even in the absence of a magnetic field (zero Zeeman splitting), we can have a non-zero linear polarization signal, simply because the number of σ transitions per unit volume and time will be larger than the number of π transitions.

On the other hand, whenever the Zeeman splitting is a very small fraction of the spectral line width, spectral lines with $J_l = 1$ and $J_u = 0$ can produce linear polarization *only* if population imbalances exist among the magnetic sublevels of their *lower-level*. If this is the case, then linear polarization can be generated via the *selective absorption* resulting from the population imbalances of the lower level (Trujillo Bueno & Landi Degl’Innocenti 1997; Trujillo Bueno 1999, 2001; Trujillo Bueno et al. 2002a; Manso Sainz & Trujillo Bueno 2003).

In summary, spectral line polarization can be produced by the mere presence of *atomic level polarization*, i.e., by the existence of population imbalances among the sublevels pertaining to the upper and/or lower atomic levels involved in the line transition under consideration. Upper-level polarization implies *sources* of polarization (through the ensuing selective emission processes), while lower-level polarization produces *sinks* of polarization (through the ensuing selective absorption processes).

3.5. THE QUANTUM DESCRIPTION: OPTICAL PUMPING

What is the key physical mechanism that induces atomic level polarization in an astrophysical plasma? The answer lies in *the anisotropic illumination of the atoms*. This is easy to understand by considering the academic case of a unidirectional unpolarized light beam that illuminates a gas of two-level atoms with $J_l = 0$ and $J_u = 1$ and that is propagating along the direction chosen as the quantization axis of the total angular momentum. Since these atoms can only absorb ± 1 units of angular momentum from the light beam, only transitions corresponding to $\Delta M = \pm 1$ are effective, so that no transitions occur to the $M = 0$ sublevel of the upper level. Thus, in the absence of any relaxation mechanisms, the upper-level sublevels with $M = 1$ and $M = -1$ would be more populated than the $M = 0$ sublevel.

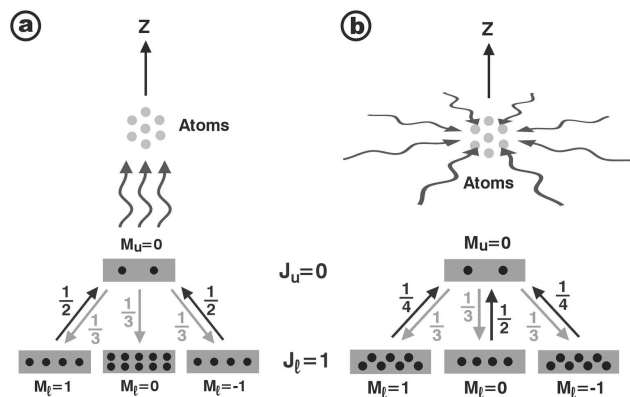


Figure 7. Illustration of the atomic polarization that is induced in the lower level of a two-level atom (with $J_l = 1$ and $J_u = 0$) by two types of anisotropic illuminations (a and b). The incident radiation field is assumed to be unpolarized and with axial symmetry around the vertical direction, which is our choice here for the quantization axis of total angular momentum. In both cases, an excess population tends to build up in the weakly absorbing sublevels. Note that the alignment coefficient of the lower level (i.e. $\rho_0^2 = (N_1 - 2N_0 + N_{-1})/\sqrt{6}$, N_i being the populations of the magnetic sublevels) is negative in case (a) (where the incident beam is parallel to the quantization axis), but positive in case (b) (where the incident beams are perpendicular to the quantization axis). The physical understanding of the information provided in this figure is left as an exercise to the reader.

Upper-level selective population pumping occurs when some *upper state* sublevels have more chance of being populated than others. On the contrary, as illustrated in Fig. 7, lower-level selective depopulation pumping occurs when some *lower state* sublevels absorb light more strongly than others. As a result, an excess population tends to build up in the weakly absorbing sublevels (Kastler 1950; Happer 1972; Trujillo Bueno & Landi Degl’Innocenti 1997; Manso Sainz & Trujillo Bueno 2003). It is also important to note

that line transitions between levels having other total angular momentum values (e.g., $J_l = J_u = 1$) permit the transfer of atomic polarization between both levels via a process called *repopulation pumping* (e.g., lower-level atomic polarization can result simply from the spontaneous decay of a *polarized* upper level). The presence of a magnetic field is not necessary for the operation of such optical pumping processes, which can be particularly efficient in creating atomic polarization if the depolarizing rates from elastic collisions are sufficiently low. Figure 8 illustrates the type of anisotropic illumination in the outer layers of a stellar atmosphere.

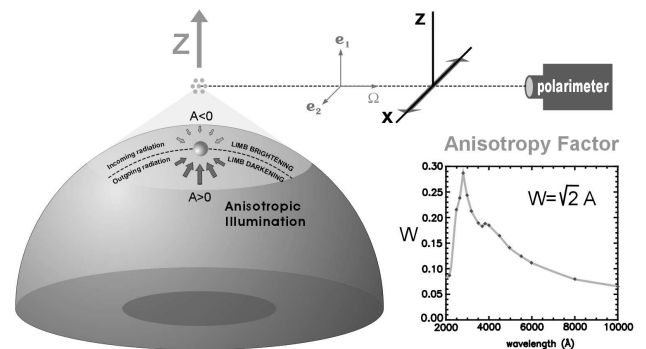


Figure 8. Anisotropic illumination of the outer layers of a stellar atmosphere, indicating that the outgoing continuum radiation shows limb darkening while the incoming radiation shows limb brightening. The figure also illustrates the type of anisotropic illumination experienced by atoms situated at a given height above the visible ‘surface’ of the star, including the polarization analysis of the scattered beam at 90° . The ‘degree of anisotropy’ of the incident radiation field is quantified by $A = J_0^2/J_0^0$, where J_0^0 is the familiar mean intensity and $J_0^2 \approx \oint \frac{d\Omega}{4\pi} \frac{1}{2\sqrt{2}} (3\mu^2 - 1) I_{\nu, \Omega}$ (with $I_{\nu, \Omega}$ the Stokes-I parameter as a function of frequency ν and direction Ω , while $\mu = \cos \theta$, with θ the polar angle with respect to the Z-axis). The possible values of the ‘anisotropy factor’ $W = \sqrt{2} A$ vary between $W = -1/2$, for the limiting case of illumination by a purely horizontal radiation field without any azimuthal dependence (case b of Fig. 7), and $W = 1$ for purely vertical illumination (case a of Fig. 7). It is important to point out that the larger the ‘anisotropy factor’ the larger the fractional atomic polarization that can be induced, and the larger the amplitude of the emergent linear polarization. We choose the positive direction for the Stokes-Q parameter along the X-axis, i.e. along the perpendicular direction to the stellar radius vector through the observed point. The inset shows the wavelength dependence of the anisotropy factor corresponding to the center to limb variation of the observed solar continuum radiation. Note that in this case the maximum anisotropy factor occurs around 2800 \AA , i.e., very near the central wavelengths of the h and k lines of Mg II, whose polarization may contain valuable information on the magnetic fields of the transition region from the chromosphere to the 10^6 K solar coronal plasma.

3.6. THE QUANTUM DESCRIPTION: COHERENCES

To understand what the Hanle effect is from a quantum mechanical point of view we need to recall first the concept of quantum coherence ($\rho_J(M, M')$) between different magnetic sublevels M and M' pertaining to each J -level. We say that the quantum coherence $\rho_J(M, M')$ is non-zero when the wave function presents a well defined phase relationship between the pure quantum states $|JM\rangle$ and $|JM'\rangle$. It is actually very common to find non-zero coherences while describing the excitation state of an atomic or molecular system under the influence of a pumping radiation field. Let us consider again a two-level atom with $J_l = 0$ and $J_u = 1$ that is being irradiated by an *unpolarized* radiation beam. In the absence of magnetic fields, all coherences of the upper level are zero *if* the quantization axis of total angular momentum is chosen along the symmetry axis of the incident radiation beam. The same happens if a magnetic field is aligned with the quantization axis and this axis coincides with the symmetry axis of the radiation field that ‘illuminates’ the atomic system. This is because unpolarized radiation propagating along the quantization axis can only produce *incoherent* excitation of the upper-level sublevels with $M = \pm 1$.⁴ If we now rotate the original reference system so that the new quantization axis for total angular momentum forms a non-zero angle with the symmetry axis of the radiation field, then non-zero coherences arise in this new reference system, even in the absence of a magnetic field. As we shall see below, a magnetic field *modifies* such quantum coherences through the Hanle effect.

We thus see that the most general description of the excitation state of a J -level requires $(2J + 1)^2$ quantities: the individual populations ($\rho_J(M, M)$) of the $(2J + 1)$ sublevels and the degree of quantum coherence between each pair of them ($\rho_J(M, M')$). These quantities are nothing but the diagonal and non-diagonal elements of the *atomic density matrix* associated with the J -level, as given by the standard representation. Alternatively, we can use the multipole components (ρ_Q^K) of the atomic density matrix, which are given by linear combinations of $\rho_J(M, M')$. The ρ_Q^K elements with $Q = 0$ are *real* numbers given by linear combinations of the populations of the various Zeeman sublevels corresponding to the level of total angular momentum J . The total population of the atomic level is quantified by $\sqrt{2J + 1}\rho_0^0$, while the population imbalances among the Zeeman sublevels are quantified by ρ_0^K (e.g., $\rho_0^2(J = 1) = (N_1 - 2N_0 + N_{-1})/\sqrt{6}$ and $\rho_0^1(J = 1) = (N_1 - N_{-1})/\sqrt{2}$). However, the ρ_Q^K elements with $Q \neq 0$ are *complex* numbers given by linear combinations of the *coherences* between Zeeman sublevels whose magnetic quantum numbers differ by Q (e.g., $\rho_2^2(J = 1) = \rho(1, -1)$). These multipole components of

⁴ Note that an unpolarized radiation beam may be considered as the incoherent superposition of right-handed and left-handed circular polarization.

the atomic density matrix provide the most useful way of quantifying, at the atomic level, the information we need for calculating the *sources* and *sinks* of polarization.

The Hanle effect is the modification of the atomic-level polarization (and of the ensuing observable effects on the emergent Stokes profiles Q and U) caused by the action of a magnetic field *inclined* with respect to the symmetry axis of the pumping radiation field. The quantum mechanical description of the Hanle effect can be suitably summarized by the following equation (Landi Degl’Innocenti & Landolfi 2004):

$$\rho_Q^K(J_u) = \frac{1}{1 + iQ\Gamma_u} [\rho_Q^K(J_u)]_{B=0}, \quad (3)$$

where $\Gamma_u = 8.79 \times 10^6 B g_{J_u}/A_{ul}$ (with B in gauss and A_{ul} in s^{-1}) and $[\rho_Q^K(J_u)]_{B=0}$ are the ρ_Q^K elements for the non-magnetic case defined in the reference frame in which the quantization axis is aligned with the magnetic field vector. This equation shows clearly that *in the magnetic field reference frame* the population imbalances (i.e., the ρ_Q^K elements with $Q = 0$) are unaffected by the magnetic field, while the ρ_Q^K elements with $Q \neq 0$ are *reduced* and *dephased* with respect to the non-magnetic case.

3.7. SUMMARIZING: GOOD NEWS VS. BAD NEWS

The good news about the Hanle effect are the following:

1. It is sensitive to magnetic fields for which the Zeeman splitting in frequency units is comparable to the inverse lifetime of the upper (or lower) level of the spectral line used, regardless of how large the line width due to Doppler broadening is. It is therefore sensitive to weaker magnetic fields than the Zeeman effect: from at least milligauss to hundreds of gauss.
2. It is sensitive to the presence of hidden, mixed-polarity fields at sub-resolution scales.
3. Contrary to a widespread belief, the diagnostic use of the Hanle effect is *not* limited to a narrow solar limb zone. In particular, in forward scattering at disk center, the Hanle effect can create linear polarization, when in the presence of inclined magnetic fields.

The downside of the Hanle effect is that it is properly a quantum effect, and the quantum theory of polarization is a complicated subject. However, it has been recently described in great detail in a rigorous monograph (see Landi Degl’Innocenti & Landolfi 2004). And we know how to solve the relevant equations accurately and efficiently in order to model polarization phenomena in (magnetized) astrophysical plasmas (e.g., the review by Trujillo Bueno 2003a).

4. HOW TO “MEASURE” THE CORONAL MAGNETIC FIELD?

The solar corona is a very effective emitter of Lyman α radiation (Gabriel et al. 1971; Kohl et al. 1980). Such a radiation results from the resonance scattering of disk Lyman

α photons by residual coronal neutral hydrogen (Gabriel 1971). This conclusion has led some authors to propose the Hanle effect in the Lyman α line as a diagnostic of the strength and direction of coronal magnetic fields between approximately 1 and 3 solar radii from sun center (Bommier & Sahal-Br  chot 1982; Fineschi et al. 1992). Obviously, this refers to the 90° scattering case.

On the other hand, the intensity profiles of the hydrogen lines of the Lyman series have been measured on the solar disk by several instruments on board rockets and space telescopes (e.g., by the SUMER spectrometer on SOHO), showing that such lines are in emission at all positions and times and that they originate in the upper chromosphere and transition region (e.g., Warren et al. 1998). Therefore, it is of great interest to investigate the diagnostic potential of the Hanle effect in the hydrogen lines of the Lyman series for the forward scattering case (Casini & Trujillo Bueno 2005; in preparation).

Interestingly, the scattering polarization of the hydrogen lines of the Lyman series are sensitive (via the Hanle effect) to the typical magnetic strengths expected for the solar outer atmosphere (chromosphere, transition region and corona). According to Eq. (1), the critical magnetic fields of the hydrogen lines of the Lyman series are approximately the following:

$$\begin{aligned} Ly_\alpha (1216\text{\AA}) &\rightarrow B_H = 50 \text{ gauss} \\ Ly_\beta (1025\text{\AA}) &\rightarrow B_H = 20 \text{ gauss} \\ Ly_\gamma (972\text{\AA}) &\rightarrow B_H = 8 \text{ gauss} \\ Ly_\delta (950\text{\AA}) &\rightarrow B_H = 4 \text{ gauss} \\ Ly_\epsilon (937\text{\AA}) &\rightarrow B_H = 2 \text{ gauss} \end{aligned}$$

In the following subsections we are going to show the expected polarization signal from the Hanle effect of the Lyman α line, both for the 90° and forward scattering cases. It is important to recall that the Lyman α line results from transitions between a lower term, $1s^2S_{1/2}$ (which has a single level with $J = 1/2$), and an upper term, $2p^2P_{1/2,3/2}$ (which has two levels with $J = 1/2$ and $J = 3/2$)⁵. We point out that the splitting between the upper levels $2p^2P_{1/2}$ and $2p^2P_{3/2}$ is of the order of 10^{10}s^{-1} , which is much larger (about 15 times) than the natural broadening of the line (of the order of $6 \times 10^8\text{s}^{-1}$). It follows that quantum interferences between these two J -levels can be neglected and the two levels can be considered as independent, at least for the particular case of an *optically thin* medium. Therefore, the Land   factor to be used in Eq. (1) for estimating the critical Hanle field of the Lyman α line is the ‘‘usual’’ one that can be obtained via the LS coupling formula. This gives $g_L = 4/3$ for the upper level $2p^2P_{3/2}$, which is the only level that contributes to the linear polarization produced by scattering processes

⁵ The other level with principal quantum number $n = 2$ (i.e., $2s^2S_{1/2}$) is of no interest here because it cannot be excited from the lower level, as long as the possible role of electric fields in the corona can be neglected.

in the Lyman α line when the hyperfine splitting (HFS) is neglected.

As we just mentioned, all previous considerations apply when HFS is neglected. However, the splitting of the two HFS-levels ($F = 1$ and $F = 2$) arising from the fine structure level $2p^2P_{3/2}$ is small ($0.237 \times 10^8\text{s}^{-1}$ -that is, about 26 times smaller than the natural width). Therefore, in agreement with the numerical calculations of Bommier & Sahal-Br  chot (1982), we conclude that HFS can be safely neglected for the modeling of the Hanle effect in the Lyman α line.

In any case, our illustrative examples below have been carried out applying the quantum theory of polarization for the *multiterm atom* with HFS in the presence of a magnetic field, as formulated by Casini & Manso Sainz (2005). Therefore, we have taken into account not only HFS, but also quantum interferences between the F -levels, even between those belonging to different J -levels within the same term. Although as confirmed by our numerical simulations for a realistic hydrogen model atom such refinements are not important for the Lyman α line, they cannot in general be neglected for modeling the Hanle effect for other hydrogen lines.

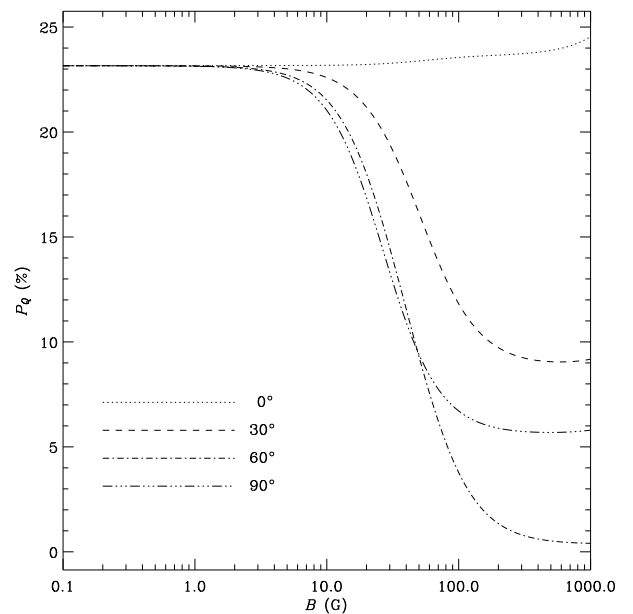


Figure 9. Theoretical estimate of the linear polarization produced by 90° scattering processes in the Lyman α line and taking into account the Hanle effect caused by the presence of a random-azimuth magnetic field with the indicated inclination. The model calculations correspond to a height of 1.5 solar radii above the solar visible surface. Note how the integrated fractional linear polarization of the Lyman α line decreases as the magnetic strength of the inclined field is increased.

4.1. 90° SCATTERING

Figure 9 shows that the linear polarization produced by scattering processes in the Lyman α line is of the order of 20% at a height of 1.5 solar radii above the visible solar surface. Interestingly, this polarization is efficiently reduced in the presence of an inclined magnetic field. As expected, the optimum sensitivity takes place for field strengths between 10 and 100 gauss, approximately.

4.2. FORWARD SCATTERING

Figure 10 shows an example of the linear polarization signal created by the Hanle effect of a horizontal magnetic field in the Lyman α line. These forward scattering polarization signals offer a novel diagnostic tool for the empirical investigation of chromospheric and coronal fields.

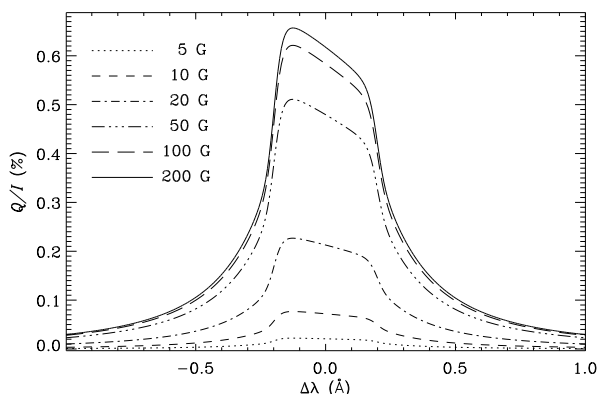


Figure 10. Theoretical estimate of the linear polarization created by the Hanle effect in the Lyman α line as a result of forward scattering processes in the presence of a horizontal magnetic field in the solar transition region. Note that the Q/I amplitude increases with the strength of the magnetic field, up to the Hanle-effect saturation field intensity (~ 200 gauss for the forward scattering case in the presence of a horizontal field). The calculations have been carried out assuming a slab of hydrogen atoms at a height of 3000 Km above the solar visible surface and neglecting the contribution of the center-to-limb variation of the Lyman α radiation on the anisotropy factor.

5. CONCLUDING REMARKS

Our response to ESA's call for themes for 2015-2025 was motivated by our belief that the polarization of electromagnetic radiation is the key to unlocking new discoveries in astrophysics. A particularly relevant example concerns cosmic magnetic fields, whose detection and quantification cannot be achieved via conventional spectroscopy, except in very particular cases.

For obvious reasons, it is convenient to distinguish between the following two scientific goals for the exploration of polarimetric signals from space.

1. The Magnetism of the Solar Corona

In our opinion, the greatest future challenge in solar physics is the empirical investigation of the magnetic field vector in the solar transition region and corona. The fundamental role played by the magnetic field in the physics of the solar corona has been widely recognized for a long time. Yet, the absolute lack of reliable measurements of the intensity and orientation of coronal magnetic fields is an extremely serious handicap for our understanding of the physical mechanisms that are responsible for the equilibrium and evolution of coronal structures.

The most promising diagnostic tool for mapping the magnetic fields of the solar transition region and corona is the Hanle effect in permitted UV lines, which requires that a development like a UV/EUV polarimeter in space be made⁶. In fact, it is believed, on the basis of very sound physical arguments, that the Hanle effect can operate, in the solar corona and transition region, in the hydrogen lines of the Lyman series, as well as in other UV emission lines of O VI, N V and C IV. These spectral lines are among the few permitted (i.e. not forbidden) lines from the transition region and corona, which are excited by the radiation coming from the solar disk. Therefore, we can predict that these lines must be polarized by scattering, and that their polarization must be modified by the presence of magnetic fields in a predictable way.

It is important to point out that the feasibility of UV polarization measurements from space has been already demonstrated, concerning both the Lyman α line (Stenflo et al. 1980) and the O VI line at 1032 Å (Raouafi et al. 1999). The immediate, next crucial step *now* is to put a high-sensitivity UV/EUV polarimeter in a solar space telescope.

Finally, we must emphasize that the UV/EUV spectropolarimetric signatures from other stars and astronomical objects remain basically unknown. The Sun can (and must) be viewed, once again, as a Rosetta stone for astrophysics.

2. Astrophysical Spectropolarimetry

The application of spectropolarimetry to other fields of astrophysics is still in an early stage of development. However, it is becoming increasingly attractive (see *Astrophysical Spectropolarimetry*, edited by Trujillo Bueno et al. 2002c). In fact, it is currently believed that the polarization of electromagnetic radiation provides the clue to the understanding of many of the astrophysical phenomena that we observe with our increasingly larger telescopes. Particularly relevant examples, besides the Sun

⁶ We point out that for the forbidden lines in the visible and near-IR the critical Hanle field given by Eq. (1) is extremely small and the corresponding linear polarization signals do not have any sensitivity to the strength of the coronal fields.

and peculiar A- and B-type stars, are young stellar objects and their surrounding disks, symbiotic stars, stellar winds, supernovae, active galactic nuclei, black-hole jets, magnetized neutron stars, X-ray pulsars, the interstellar medium, astronomical masers, the cosmic microwave background radiation and its cosmological implications, etc.

Our scientific suggestion in this respect is to carry out detailed observational explorations of spectral line polarization signals in a variety of astronomical objects throughout the whole spectrum, but mostly in the UV/EUV spectral region. The best way to carry out this type of explorations is from a space telescope. The necessary instrumentation should be designed in order to be able to detect weak polarization signals, of the order of 10^{-4} in fractional polarization. Interestingly, scattering polarization is able to provide geometrical information on scales that could never be spatially resolved directly at optical or IR wavelengths, even with the largest telescopes.

We bear no doubt that spectropolarimetry will be a revolutionary technique in 21st century astrophysics. ESA should take advantage of the present European leadership in this field to open this new diagnostic window on the Universe.

ACKNOWLEDGEMENTS

This work has been partially supported by the Spanish Ministerio de Educación y Ciencia through project AYA2004-05792 and by the European Solar Magnetism Network.

REFERENCES

- Asensio Ramos, A., Landi Degl'Innocenti, E., Trujillo Bueno, J. 2005, ApJ, 625, 985
- Bohr, N. 1924, Naturwissenschaften, 12, 1115
- Bommier, V., Sahal-Bréchet, S. 1982, Solar Phys. 78, 157
- Bommier, V., Landi Degl'Innocenti, E., Leroy, J. L., Sahal-Bréchet, S. 1994, Solar Phys. 154, 231
- Born, M., & Wolf, E. 1994, *Principles of Optics*, Pergamon Press, Oxford
- Casini, R., Manso Sainz, R. 2005, ApJ, 624, 1025
- Casini, R., López Ariste, A., Tomczyk, S., Lites, B. W. 2003, ApJ, 598, L67
- Collados, M., Trujillo Bueno, J., Asensio Ramos, A. 2003, in Solar Polarization 3, eds. J. Trujillo Bueno & J. Sánchez Almeida, ASP Conf. Series 307, 468
- Fineschi, S. et al. 1992, SPIE Vol. 1742, 423
- Gabriel, A. H. 1971, Solar Phys., 21, 392
- Gabriel, A. H., et al. 1971, ApJ, 169, 595
- Gandorfer, A. 2000, *The Second Solar Spectrum*, Vol. 1: 4625 Å to 6995 Å ISBN 3 7281 2764 7 (Zürich: vdf)
- Gandorfer, A. 2002, *The Second Solar Spectrum*, Vol. 2: 3910 Å to 4630 Å ISBN 3 7281 2855 4 (Zürich: vdf)
- Hanle, W. 1924, Z. Phys., 30, 93
- Happer, W. 1972, Rev. Mod. Phys., 44, 169
- Heisenberg, W. 1925, Z. Phys., 31, 617
- Kastler, A. 1950, J. de Physique, 11, 255
- Kohl, J. L. et al. 1980, ApJ Letters, 241, L117
- Lagg, A., Woch, J., Krupp, N., Solanki, S. 2004, A&A, 414, 1109
- Landi Degl'Innocenti, E., 1998, Nature, 392, 256
- Landi Degl'Innocenti, E., Landolfi, M. 2004, *Polarization in Spectral Lines*, Kluwer Academic Publishers
- Manso Sainz, R., Trujillo Bueno, J. 2003, Phys. Rev. Letters, 91, 111102-1
- Merenda, L., Trujillo Bueno, J., Landi Degl'Innocenti, E., Collados, M. 2005, ApJ, submitted
- Moruzzi, G., Strumia, F. (eds.) 1991, *The Hanle Effect and Level-Crossing Spectroscopy*, New York: Plenum
- Raouafi, N. E., Lemaire, P., Sahal-Bréchet, S. 1999, A&A, 345, 999
- Solanki, S. K., Lagg, A., Woch, J., Krupp, N., Collados, M. 2003, Nature, 425, 692
- Stenflo, J.O. 1994, *Solar Magnetic Fields: Polarized Radiation Diagnostics*, Kluwer Academic Publishers
- Stenflo, J. O. et al. 1980, Solar Phys., 66, 13
- Stenflo, J. O., Keller, C. 1996, Nature, 382, 588
- Trujillo Bueno, J. 1999, *Towards the Modelling of the Second Solar Spectrum*, in Solar Polarization, eds. K. N. Nagendra and J. O. Stenflo, Kluwer Academic Publishers, 73
- Trujillo Bueno, J. 2001, *Atomic Polarization and the Hanle Effect*, in Advanced Solar Polarimetry: Theory, Observation and Instrumentation, ed. M. Sigwarth, ASP Conf. Series 236, 161
- Trujillo Bueno, J. 2003a, *The Generation and Transfer of Polarized Radiation in Stellar Atmospheres*, in Stellar Atmosphere Modeling, eds. I. Hubeny, D. Mihalas and K. Werner, ASP Conf. Series 288, 551
- Trujillo Bueno, J. 2003b, *New Diagnostic Windows on the Weak Magnetism of the Solar Atmosphere*, in Solar Polarization 3, eds. J. Trujillo Bueno & J. Sánchez Almeida, ASP Conf. Series 307, 407
- Trujillo Bueno, J., Landi Degl'Innocenti, E. 1997, ApJ Letters, 482, L183
- Trujillo Bueno, J., Landi Degl'Innocenti, E., Collados, M., Merenda, L. & Manso Sainz, R. 2002a, Nature, 415, 403
- Trujillo Bueno, J., Casini, R., Landolfi, M., Landi Degl'Innocenti, E. 2002b, ApJ Letters, 566, L53
- Trujillo Bueno, J., Moreno-Insertis, F., Sánchez, F. (eds.) 2002c, *Astrophysical Spectropolarimetry*, Cambridge University Press
- Trujillo Bueno, J., Shchukina, N., Asensio Ramos, A. 2004, Nature, 430, 326
- Trujillo Bueno, J., Merenda, L., Centeno, R., Collados, M., Landi Degl'Innocenti, E. 2005, ApJ Letters, 619, L191
- Warren, H.P., Mariska, J.T., Wilhelm, K. 1998, ApJS, 119, 105